Annals of the Academy of Romanian Scientists
Series on Engineering Sciences
ISSN 2066 – 8570 Volume **6**, Number **2**/**2014**

WHAT LINK BETWEEN CHIP ORIENTATION AND MOMENT AT THE TOOL TIP POINT IN TURNING?

Olivier CAHUC[1], Miron ZAPCIU[2], Claudiu BISU[3], Alain GERARD[4]

Rezumat. *De câțiva ani, a fost realizată o mai bună înțelegere a procesului de așchiere a materialelor, beneficiind de posibilitatea măsurării forțelor și a momentelor. În acest articol, au fost măsurate simultan șase componente mecanice, trei forțe și trei momente, precum și măsurători de orientare a așchiilor în timpul testelor de strunjire. În timpul acestor teste a fost observată influența adâncimii de așchiere și a vitezei de avans și a fost demonstrată corespondența între orientarea așchiilor și orientarea momentul vector sau caracteristicile axei centrale a prelucrării.*

Abstract. *Since some years, the better understanding of the material cutting process has been shown with the benefit of the forces and moments measurement. In this article, simultaneous six mechanical components and chip orientation measurements were realized during turning tests. During these tests, the influence of the depth of cut or feed rate has been observed and correlation between the chip orientation and the moment vector orientation or the central axis characteristics has been shown.*

Keywords: Manufacturing, Torsor measurement, Chip orientation, Central axis

1. Nomenclature

ap	Depths of cut (mm)
BT	Block Tool
BW	Block Workpiece
D_1	Holding fixture diameter (mm)
D_2	Workpiece diameter (mm)
E	Young modulus (N/mm^2)
F_i	Force components vector (i = x, y, z) [N]
F_c	Cutting force [N]
F_a	Feed force [N]
F_p	Radial force [N]
f	feed rate (mm/rev)
L_1	Holding fixture length (mm)
L_2	Length workpiece (mm)
M_i	Moment components vector (i = x, y, z) [dNm]

[1]Prof., University of Bordeaux and CNRS UMR 5295, I2MI Département MPI, University, 351 cours de la Libération 33405 Talence FRANCE (olivier.cahuc@u-bordeaux1.fr).
[2]Prof., University Politehnica of Bucharest, Corresponding member of Academy of Romanian Scientists, Spl. Independentei, no. 54. Bucharest, Romania (miron.zapciu@upb.ro).
[3]Associate Prof., University Politehnica of Bucharest, Machines and Production Systems department, Spl. Independentei, no.313. Bucharest, Romania (claudiu.bisu@upb.ro).
[4]Prof., University of Bordeaux and CNRS UMR 5295, I2MI Département MPI, University, 351 cours de la Libération 33405 Talence FRANCE (alain.gerard@u-bordeaux1.fr).

Vc	Cutting speed (m/min)
WTM	Workpiece-Tool-Machine
x (z)	Cross (feed) direction
y	Cutting axis
α	Clearance angle
γ	Cutting angle
λ_s	Angle of edge
κ_r	Direct angle
r_ε	Nozzle radius (mm)
R	Sharpness radius

2. Introduction

Metal cutting is one of the most important manufacturing processes. The most common cutting processes are turning, milling, drilling and grinding. During the cutting process of different materials, a whole of physic-chemical and dynamic phenomena are involved. Elasto-plastic strains, friction and thermal phenomena are generated in the contact zone between workpiece, tool and chip. These phenomena are influenced by: physical properties of the materials (workpiece and tool), tool geometry, cutting and lubrication conditions, and also the machining system dynamic parameters (stiffness, damping). The machine tool vibrations are generated by the interaction between the elastic machining system and the cutting process. The elastic system is composed of: the different parts of the machine tool in movement, the workpiece and the tool. Actions of the machining process are usually forces and moments. These actions also generate relative displacements of elements composing the elastic system [1]. They occur for example between the tool and workpiece, the tool device and bed, etc. These displacements modify the cutting conditions and in the same way the mechanical actions [2]. Thus, the knowledge of the machining system elastic behaviour is essential to understand the cutting process [3, 4]. In these processes, the cutting forces measurement has important and tremendous applications within industry and research alike [5]. The cutting forces estimation allows to supervise tool wear evolution [6], establishes material machinabilities, optimizes cutting parameters, predicts machined workpiece surface quality and study phenomena such as chip formation or vibrations appearance. Knowing the cutting forces is essential to machine tool builders in calculating power requirements and frame rigidity [7]. Cutting forces acting on the tool must be measured at the design tool that are strong enough to remove chip [8] at the desired quantity from the workpiece and to calculate power of tool driver system. The dynamometer is able to measure three force components: cutting force (F_c), feed force (F_a) and radial force (F_p) but not the torque at the tool tip. Axinte et al., [9, 10] propose a procedure to account for both calibration and process errors in the uncertainty estimation for the specific situation of single cutting force measurements [11].

However the dynamometer can measure three perpendicular cutting force components and three torque components simultaneously during turning, and the measured numerical values can be stored in computer by data acquisition system [12]. This dynamometer was designed to measure up to 5,000 N maximum force and 350 dN/m torque. The system sensitivity is ± 4% in force and ± 6% in torque.

3 Experimental device

Fig. 1. Lathe RTN30

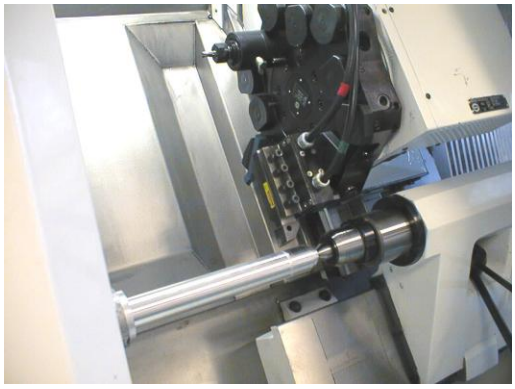

Fig. 2. Experimental machining system and metrology environment in turning process

Dynamic cutting tests are carried out on a lathe Ramo (RTN30) for which the spindle speed does not exceed 6000 rpm (Fig. 1). The main components of the test machining system used are presented without its data-processing environment in the Fig. 2. Moreover, a six-components dynamometer [13], being used as tool-holder [14], is positioned on the lathe to measure all the cutting mechanical actions (forces and torques).

The three-dimensional dynamic character is highlighted by seeking the various existing correlations between the various parts of the machining system and the various parameters evolutions, which ensure to characterize the process.

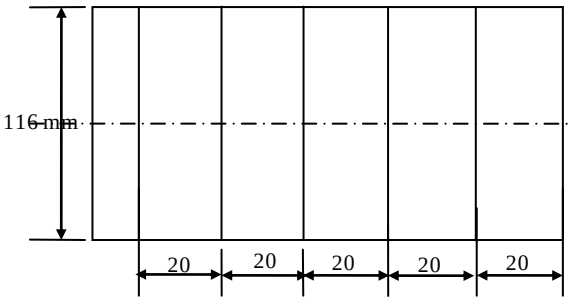

Fig. 3 Workpiece geometry for ap=3.5 mm and f variable

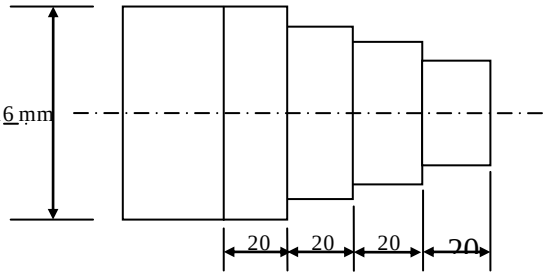

Fig. 4 Workpiece geometry for variable ap and for feed rate f=0.1 mm/rev.

The **BT** part includes the tool, the tool-holder, the dynamometer, the fixing plate on the cross slide. The six-component dynamometer [13] is fixed between the cross slide and the tool-holder (Fig. 2). This is necessary thereafter to measure the cutting mechanical actions.

An example of the measurement is given in the Fig. 5 and 6.

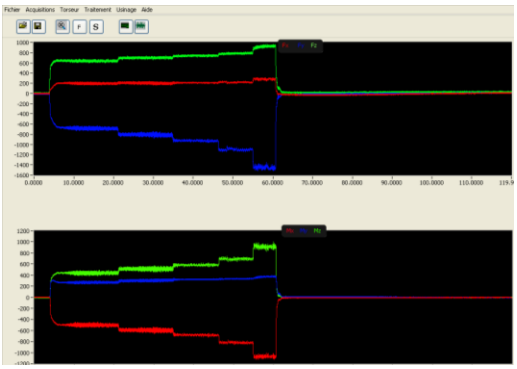

Fig. 5. Signals related to the force and moment components following the three **x**, **y**, **z** cutting directions; test case using parameters ap = 3.5 mm, f variable and Vc = 238 m/min.

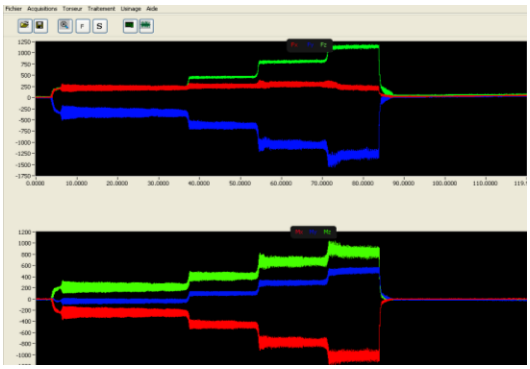

Fig. 6. Signals related to the force and moment components following the three **x**, **y**, **z** cutting directions; test case using parameters ap variable, f = 0.1 mm/rev and Vc = 238 m/min.

4 Tests results

For each test, except the feed rate or the depths of cut values, all the turning parameters are constant. The mechanical actions are measured according to the feed rate (f) using the six components dynamometer following the method developed and finalized by Couétard [14] and used in several occasions [15, 16, 17, 18, 19]. On the experimental device, (Fig. 2) the instantaneous spindle speed is permanently controlled.

During the tests the insert tool used is type *TNMA 16 04 08* carbide not covered, without chip breaker. The machined material is a steel alloy of chrome molybdenum type *42CD4T*. The test-workpieces are cylindrical with a diameter of 116 mm. They were designed starting from the Finite Elements Method being coupled to a procedure of optimization described in [20].

Moreover, the tool geometry is characterized by the cutting angle γ, the clearance angle α, the inclination angle of edge λ_s, the direct angle κ_r, the nozzle radius r_ε and the sharpness radius R [21]. The tool parameters are detailed in the Table 1.

Table 1. Geometrical characteristics of the tool

γ	α	ℓ_s	κ_r	$r_\odot$	R
-6°	6°	-6°	91°	0.8 mm	1.2 mm

5. Cutting torsor actions

5.1 Tests

For each test, the complete torsor of the mechanical actions is measured using the six-component dynamometer.

These mechanical actions are evaluated in two different configurations. The first one with constant feed rate f = 0.1 mm/rev, variable depths of cut: a_p = 1; 2; 3.5; 5 mm and the test-workpieces is cylindrical with a diameter of 116 mm.

For every value of ap the manufacturing is made with landings 20 mm in length on a cylinder beforehand prepare in staircase (Fig. 4) The second one has a different depths of cut: a_p = 3.5 mm and variable feed rate f: = 0.05; 0.0625; 0.075; 0.1; 0.15 mm/rev on the same initial diameter of 116 mm. The diameter of the cylindrical test tube is constant and every manufacturing is made on a 20 mm length (Fig. 3).

The six-component dynamometer gives the instantaneous values of all the torque cutting components in the three-dimensional space (***x***, ***y***, ***z***) related to the machine tool (Fig. 3).

Measurements are performed in O', which is the center of the six-component dynamometer. Then, they are transported to the tool point O via the moment transport classical relations. Measurement uncertainties of the six-component dynamometer are: ±4 % for the force components and ±6 % for the moment components.

5.2 Force components of the cutting actions analysis

For the first test feed rate f = 0.1 mm and four depth of cut indicated above, an example of average forces resultant measurements applied to the tool tip point are presented on Table 2.

For the five values feed rate f indicated above, one example of forces resultant measurements applied to the tool tip point is presented on Table 3.

Table 2. Average forces components measured at the tool tip point (f=0.1 m/rev)

ap [mm]	F_x [N]	F_y [N]	F_z [N)	‖R‖ [N]	M_x [dNm]	M_y [dNm]	M_z [dNm]	‖M‖ [dNm]
1	213.4	-340.8	224.7	460.6	11.1	-31.3	-28.5	43.7
2	257.6	-630	456.3	819.4	5.2	-22.7	-27.8	36.3
3.5	294.5	-1,060.3	805.1	1,363.5	9	-43.8	-62.3	76.7
5	226.1	-1,286.7	1,135.9	1,731.2	67	-104	-40.3	103.1

The analysis of Table 2 and 3 confirms the following results obtained in [22]:

$$|Fx| < |Fz| < |Fy|. \quad (1)$$

$$|M_{oz}| < |M_{oy}| < |M_{ox}|, \text{ (whatever } f\text{)}. \quad (2)$$

Table 3. Average forces components measured at the tool tip point (a_p=3.5 mm)

f [m/rev]	F_x [N]	F_y [N]	F_z [N]	‖R‖ [N]	M_x [dNm]	M_y [dNm]	M_z [dNm]	‖M‖ [dNm]
0.05	197.6	-982.7	637.3	435,087.4	5.2	- 25.8	-34	43
0.0625	202.2	-808.2	698.4	564,385.4	4.6	- 28.7	- 45.1	53.7
0.075	208.9	-926.0	738.8	684,154.9	6.1	- 33.3	- 57.3	66.6
0.1	217.3	-1,099.1	784.4	862,076.3	2.2	- 47.4	- 68.7	83.6
0.15	281.5	-1,451.6	922.3	1,338,821.9	9.8	-5 6.9	- 90.7	107,6

We notice that the absolute value of the force components case for the moment's components. As we wish to look at the sensibility of moments with diverse parameters, we restrict our investigations on the moment's evolution.

6 Moments analysis at central axis

Central axis. It is well-known that, it is possible to associate a central axis, to any torsor (except the torsor of pure moment), which is the single object calculated starting from the six torsor components [22]. A torsor $[A]_O$ in a point O is composed of the resultant forces $\boldsymbol{R}$ and the resulting moment $\boldsymbol{M_O}$.

$$A_O = \begin{Bmatrix} \vec{R} \\ \vec{M}_O \end{Bmatrix} \quad (3)$$

The central axis is the straight line classically defined by:

$$OA = \frac{\vec{R} \wedge \vec{M}_O}{\left\| R^2 \right\|} + l \vec{R} \quad (4)$$

where O is the point where the mechanical actions torsor was moved (here, the tool tip) and A the current point describing the central axis. Thus, **OA** is the vector associated with the bi-point [O, A] (Fig. 7). This line (Fig. 7 a) corresponds to the geometric points where the mechanical actions moment torsor is minimal. The central axis calculation consists in determining the point's assembly (a line) where the torsor can be expressed along a slide block (straight line direction) and the pure moment (or torque) [22].

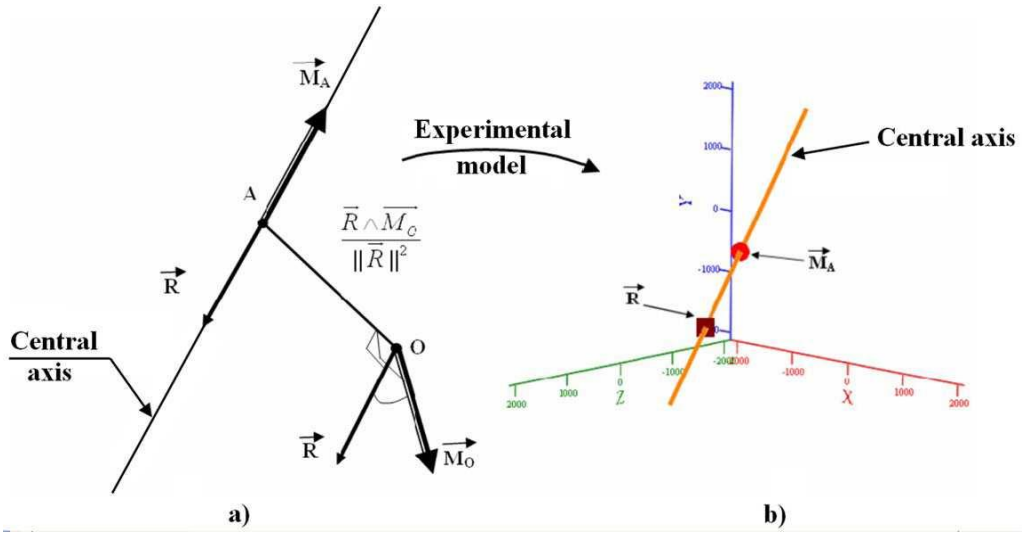

Fig. 7. Central axis representation (**a**) and of the colinearity between vector sum ***R*** and minimum moment $\boldsymbol{M}_A$ on central axis (**b**).

7. Central axes beams analysis

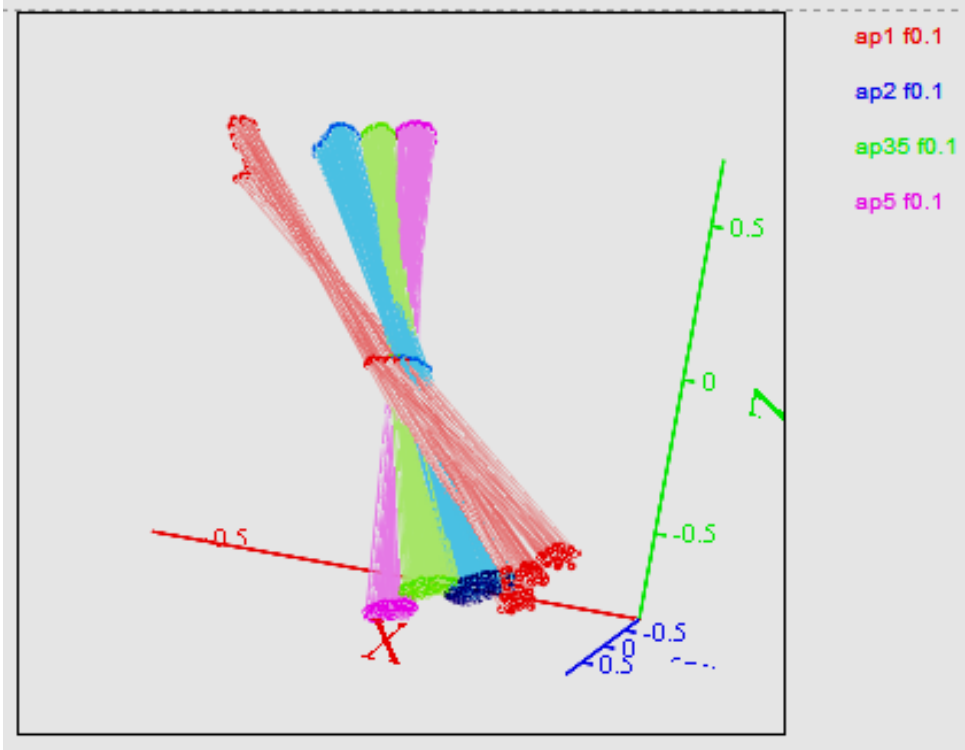

Fig. 8. Central axes beams for a_p variable, f = 0,1.

The results given to the previous paragraphs allow us to determine the central axes beams. Fig. 8 gives a representation of these in the case f = 0.1 [mm/rev] and ap variable. Also the Fig. 9 gives the evolution of the central axes in the case ap = 3.5 [mm] and variable f.

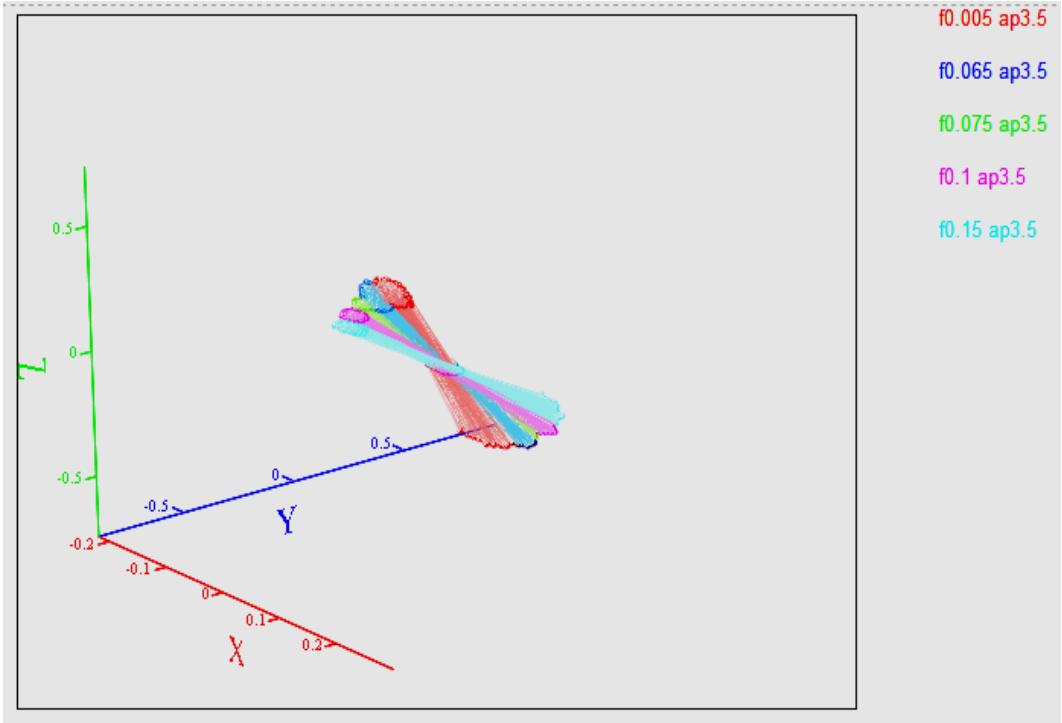

Fig. 9. Central axes beams for a_p = 3,5 mm, f variable.

In both cases, we notice the convergence of all central axes towards the same very narrow zone of elliptic shape (a quasi point) placed in a plan in agreement with [23]. This zone corresponds instead of the summits of the cones of the central axes beams, which evolve in time.

This evolution is led by the light vibrations of the system manufacturing that we can notice on the represented examples of metrology Fig. 5 and 6. Besides, considering the definition of the central axes, the narrow zone of convergence of these central axes is the place of the points where moments are minimal. But the principle of the virtual works shows that vectorials spaces efforts and movements are two dual spaces. In other words, the properties established for a vectorial space are it also for its dual space.

As a result, the properties of minimum revealing for moments are also valid for the displacements. Thus, it is the center of the rigidity (minimum place of the movements) of the system, which we so determine by another method than, that used in [24].

Furthermore we notice that when f increases, the angles of the axes of the cones of the central axes beams with regard to the axis Z increase (Fig. 10) while it decreases when a_p increase (Fig. 11).

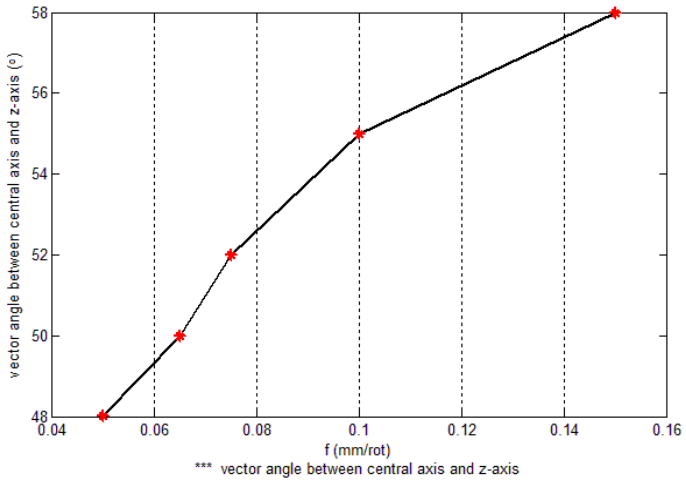

Fig. 10. Angle of the axes of the cones of the central axes with the axis Z when f increases.

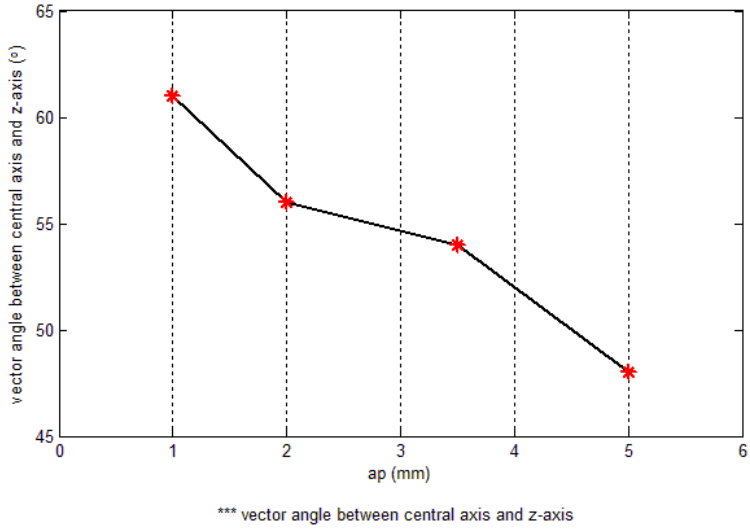

Fig. 11. Angle of the axes of the cones of the central axes with the axis Z when a_p increases.

In the case of the increasing evolution of a_p for $f = 0.1$ [mm/rev] we observe that the angular variation of the central axes with the axis Z is quasi-linear. On the other hand when f grows for a_p=3.5 [mm] the evolution of the angle of the central axes with the axis Z is almost a curve of degree 2. The evolution of the module of moments reported to the chip ejection angle is also interesting. We notice in particular that this evolution is parabolic in case a_p is increasing (Fig. 12). On the other hand, this evolution is linear when f is increasing (Fig. 13).

This analysis of the moment's module shows that it exist a rather different behavior enters the chip ejection angle in a_p growing or in increasing f. This allows us to seize better the differences observed in the behavior of the central axes beams as a_p (Fig. 8) or f (Fig. 9) is increasing.

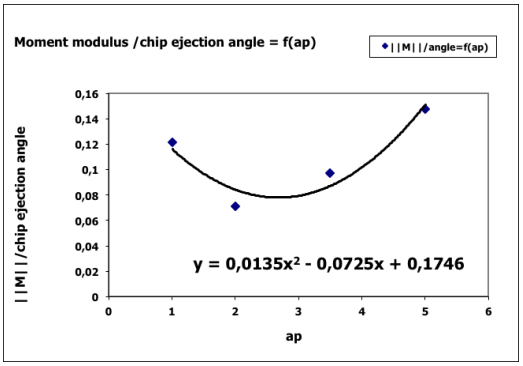

Fig. 12. Evolution of the module of moments reported to the chip ejection angle in a_p growing

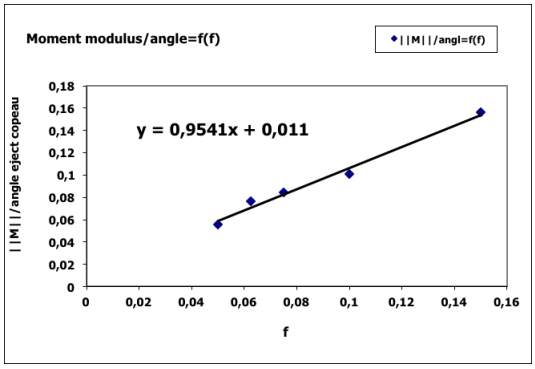

Fig. 13. Evolution of the module of moments reported to the chip ejection angle with increasing f.

8. Moment modulus analysis

Thus, we notice a slightly parabolic and always increasing evolution of the module of the moments of the efforts according to the increasing evolution of a_p for f = 0.1 [mm/rev] (Fig. 15) but also for growing f with a_p = 3.5 [mm] (Fig. 14). Only the curves concavity changes between these two series of measures. For variable f, moments seem soft towards an asymptote whereas for a_p growing the evolution is an asserted monotonous growth. We remark that the module of moment are the same order in Table 2 and 3.

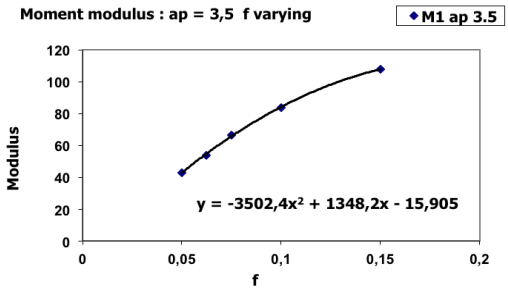

Fig. 14 Evolution of the modules of moments for a_p =3.5 [mm] and variable f.

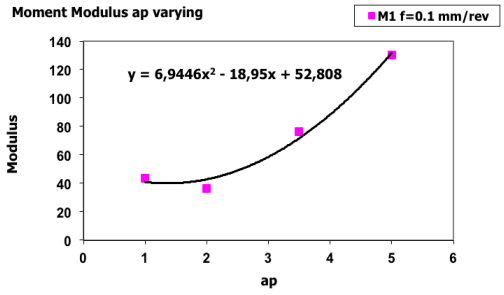

Fig. 15 Evolution of the modules of moments for f = 0.1 [mm/rev] and ap variable.

It is also interesting to look at the evolution of the chip ejection angle according to the moments module when f varies (for a_p = 3.5 [mm]; Fig. 16) and when a_p varies (f = 0.1 [mm/rev.]; Fig. 17).

We also notice that *Mx* is always positive whereas *My* and *Mz* is always negative. For a_p growing there is a minimum about 60° (Fig. 16) that is between a_p = 2 and

a_p=3.5. It is advisable to note that this minimum corresponds to a change of moments evolution; all the constituents of moments decrease until a_p = 2 then grow from a_p = 3.5. This is in agreement with the Fig. 15.

We see that moments are more sensitive than force them to these parameters. Indeed if the strengths are always increasing with a_p this is not any more the case with moments. The components of these pass by a minimum for a_p = 2. On the other hand, when f varies the component Fy and the component Mx pass by a minimum for f = 0.0625.

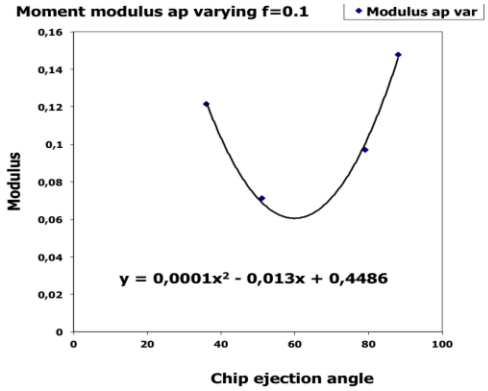

Fig. 16. Evolution of the modules of moments at the tool tip point according to the chip ejection angle and a_p growing.

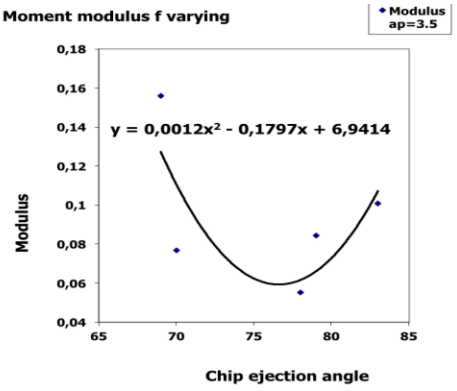

Fig. 17. Evolution of the modules of moments at the tool tip point according to the chip ejection angle and the increasing f.

Conclusion

We brought to light a simple method to determine the center of the rigidity (rotation) dynamic of the system manufacturing directly from the measure of the complete mechanical torsor of the efforts applied at the tool tip point. It is an important element that intervenes in a major way in the process of chip formation that depends on it strongly [24], [25], [26].

We notice that there is a clear correlation between the evolution of the chip ejection angle and the evolution so many moments as central axes. However the chip ejection angle seems to be more sensitive to the evolution of the moments than the resultant of the strengths led by the manufacturing. The linear evolutions (resp. parabolic) obtained enter the evolution of moments when a_p (resp. f) increases according to the chip ejection angle is an important result for the simulations of current manufacturing.

Besides evolution of the modules of the moments of the efforts reported to the chip ejection angle when f varies is linear whereas when a_p grows this evolution is parabolic. We also notice that the angle of the central axes with the axis Z is parabolic type when f increases while it is linear when it is a_p which increases.

These diverse results are important for the constitution of the simulation software of manufacturing outstanding discounted bills.

Other results of measures in the course of perusal also show the importance which there is to follow the evolution of moments in the course of manufacturing and will be presented in the next publication.

R E F E R E N C E S

[1] D.E. Dimla, J. Mater. Process Technol. **155-156** (**2004**), p. 708.

[2] C.K. Chen, Y.M. Tsao, Int. J. Adv. Manuf. Technol. **29** (**2006**), p. 649.

[3] T. Cano, F. Chapelle, J. M. Lavest,P. Ray, Int. J. Mach. Tools Manuf. **4**8, (**2008**), p. 1569.

[4] P.G. Bernados, S. Mosialos, G.C. Vosniakos, Robot Comput-Integr Manuf. **22** (**2006**), p. 505.

[5] S. Yaldiz, F. Unsacar, H. Saglam, H. Isik, Mech. Syst. Signal Process **21** (**2006**), p. 1499.

[6] C. K.Toh, MD **25**, (**2004**) 41.

[7] DE. Dimla, J. Mater Process Technol. **155-156** (**2004**), p. 1708.

[8] RJ. Lian, B.F. Lin, J.H. Huang, Int. J. Adv. Manuf. Technol. **29** (**2007**), p. 436.

[9] D. A. Axinte, W. Belluco, L.De Chiffre, Int. J. Mach. Tools Manuf. **41** (**2001**) 719.

[10] S. Yaldiz, F. Unsacar, Mater. Des. **27** (**2006**), p. 839.

[11] S. Yaldiz, F. Unsacar, Measurement **39** (**2006**), p. 80.

[12] K. Mehdi, J-F. Rigal, D. Play, J. Manuf. Sci. Eng. **124** (**2002**), p 569.

[13] Y. Couétard, Thèse de doctorat, Université Bordeaux 1 (**2000**).

[14] Y. Couétard, Y. Brevet français - CNRS- 93403025.5 N° d'ordre:2240 (**1993**).

[15] D. Toulouse, Thèse de doctorat, Université Bordeaux 1 (**1998**).

[16] O. Cahuc, P. Darnis, A. Gérard, J. L. Battaglia, In Rev. IJAMT **29** (**2001**), p. 648.

[17] Y. Couétard, O. Cahuc, P. Darnis, In: Third Int. Conf. on Met. Cut. and High Speed Machining, 27-29 juin - Metz (**2001**).

[18] P. Darnis, O. Cahuc, Y. Couétard, In: Sem. on Improv. Mach. Tool Perfor (**2000**) La baule.

[19] R. Laheurte, O. Cahuc, P. Darnis, J. L. Battaglia, 6th Int. ESAFORM (**2003**) Salerno.

[20] R. Laheurte, Thèse de doctorat, Université Bordeaux 1 (**2004**).

[21] C. F. Bisu, J. Y. K'nevez, P. Darnis, R. Laheurte, A. Gérard, Int. J. of Mat. Form. **2** (**2009**).

[22] C. F. Bisu, P. Darnis, A. Gérard, J.Y. K'nevez, Int. J. Adv. Manuf. Technol. 44, (**2009**).

[23] P. Brousse, Cours de mécanique 1er cycle et classe prépa.. Armand colin, Paris (**1973**).

[24] A.V. Dassanayake, C.S. Suh, Communic Nonlin. Sci. Num. Simul. **13** (**2008**), p. 979.

[25] Y. Sahin, A.R. Motorcu, Mater. Des. **26** (**2005**), p. 32.

[26] D.I. Laqlwani, N.K. Mehta, P.K. Jain, J. Mater Process Technol **206** (**2008**), p. 167.